Expanded View Figures

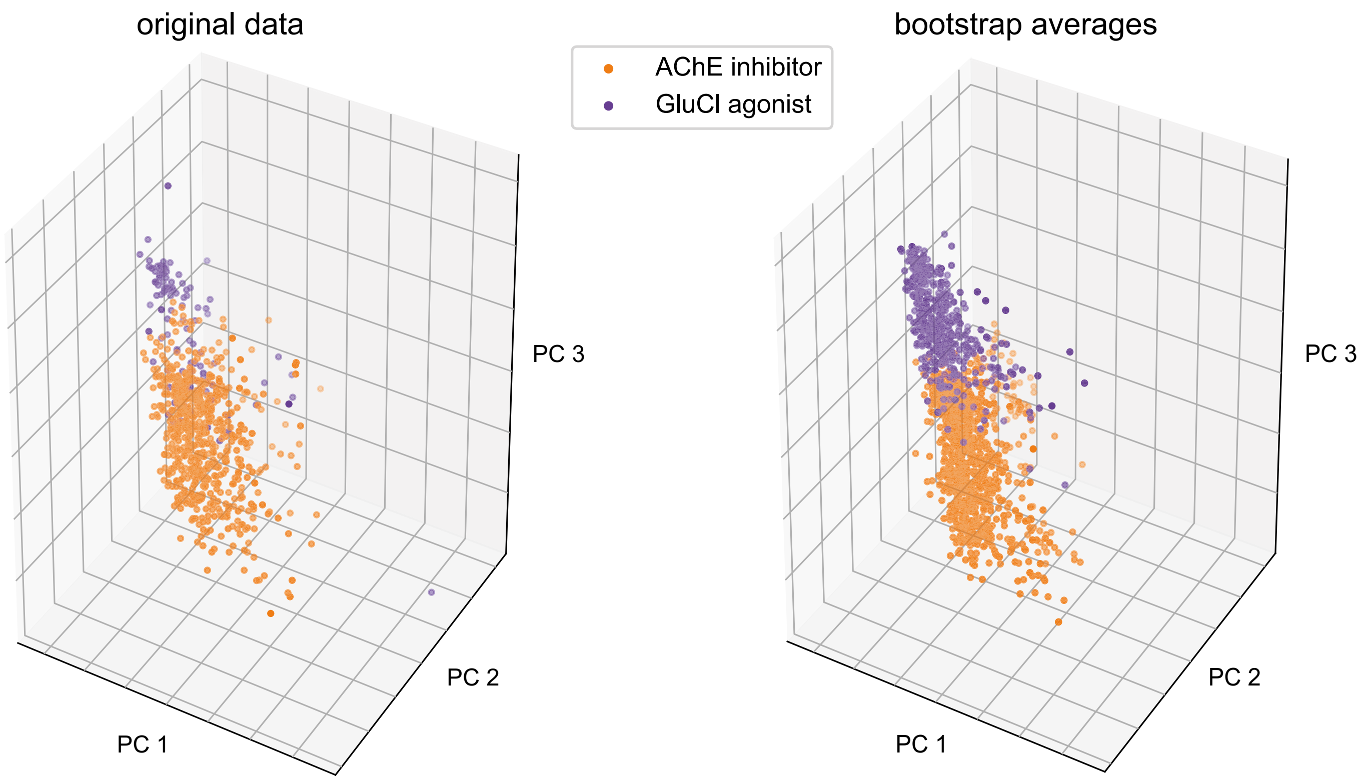

Figure EV1. The smoothing and balancing procedure using bootstrapped averages reduces the effect of outliers and balances the classes increasing classification accuracy.

One of the sparsely populated classes (GluCl agonists with 5 compounds) and the most well-populated class (AChE inhibitors with 10 compounds) are shown before and after the smoothing and balancing procedure in the 3 top PCA components.

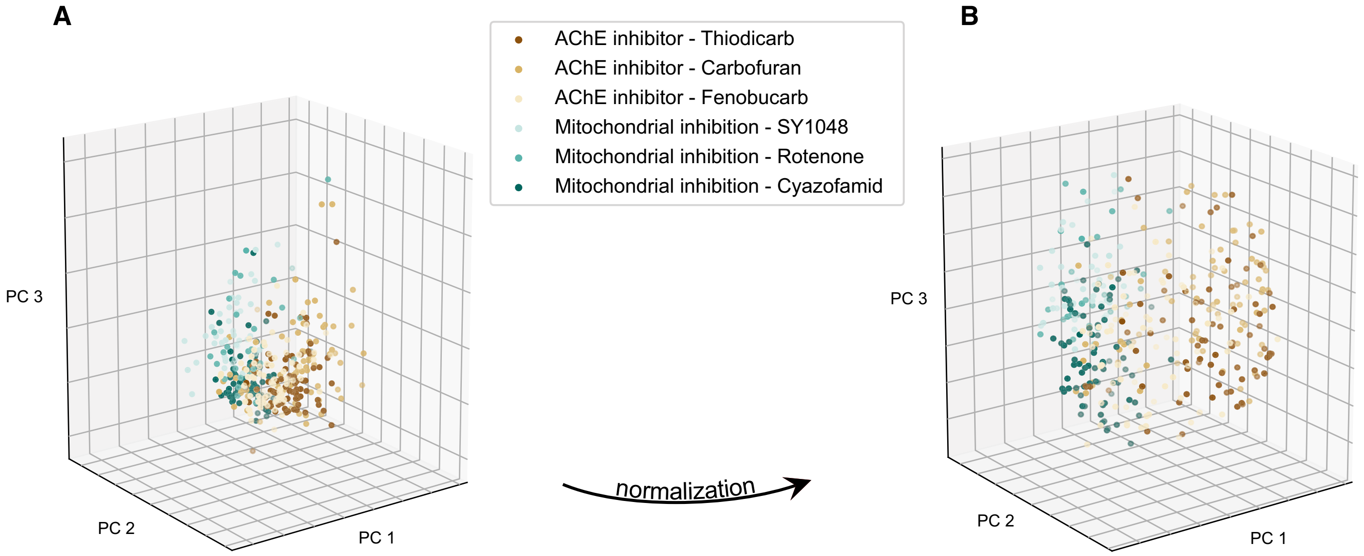

Figure EV2. Illustration of the effect of normalization with real data.

The normalization of samples to unit L2 norm brings compounds with different potencies closer together and helps separate the classes in the phenotypic space.

A PCA of the data from 2 different classes with 3 compounds each before normalization (data simply standardized).

B PCA of the normalized data.

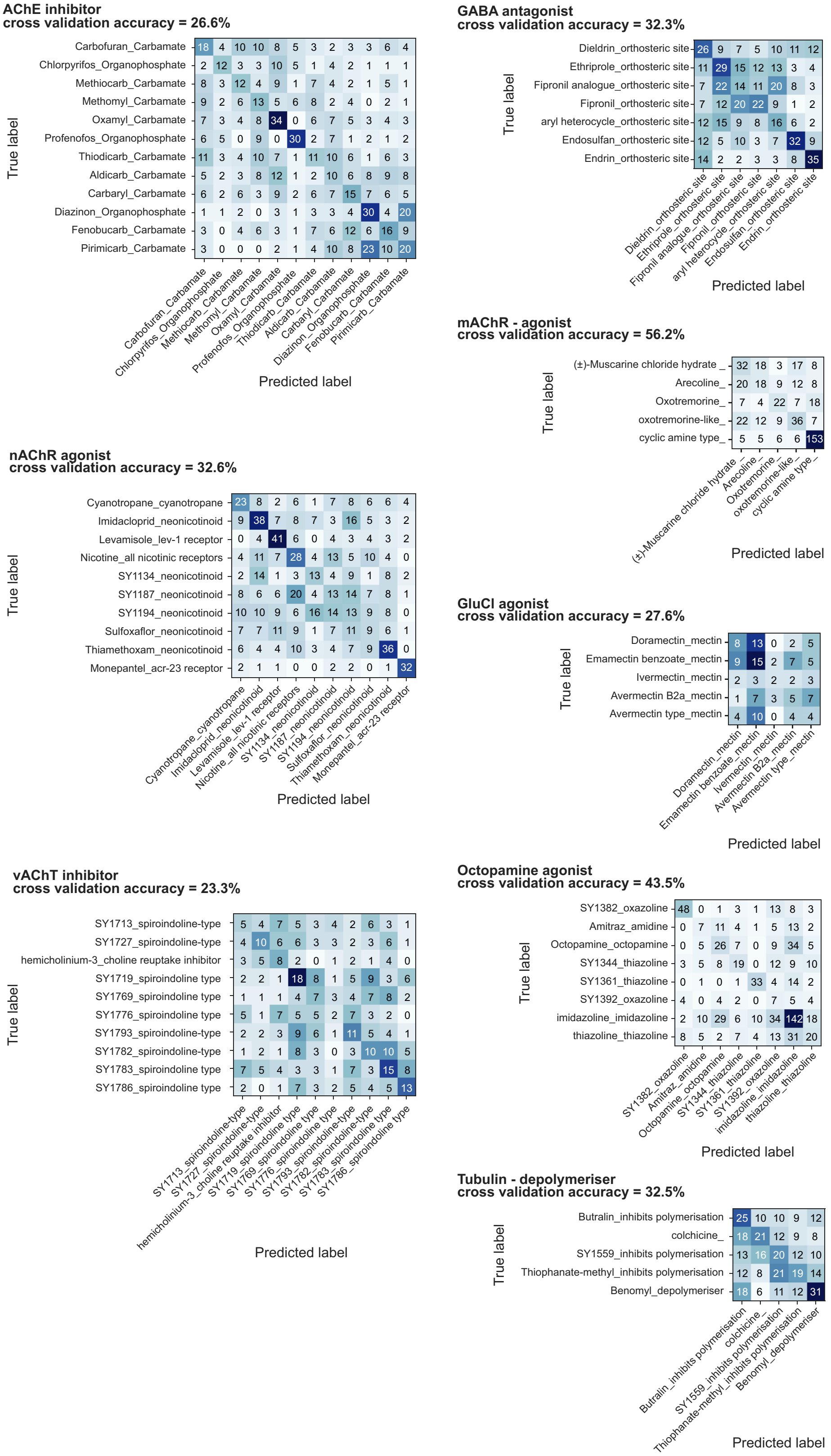

AChE inhibitor
cross validation accuracy = 26.6%

	Carbofuran_Carbamate	Chlorpyrifos_Organophosphate	Methiocarb_Carbamate	Methomyl_Carbamate	Oxamyl_Carbamate	Profenofos_Organophosphate	Thiodicarb_Carbamate	Aldicarb_Carbamate	Carbaryl_Carbamate	Diazinon_Organophosphate	Fenobucarb_Carbamate	Pirimicarb_Carbamate
Carbofuran_Carbamate	18	4	10	10	8	5	3	2	3	3	6	4
Chlorpyrifos_Organophosphate	2	12	3	3	10	5	1	4	2	1	1	1
Methiocarb_Carbamate	8	3	12	4	9	1	7	4	2	1	5	1
Methomyl_Carbamate	9	2	6	13	5	6	8	2	4	0	2	1
Oxamyl_Carbamate	7	3	4	8	34	0	6	7	5	3	4	3
Profenofos_Organophosphate	6	5	0	9	0	30	2	7	1	2	1	2
Thiodicarb_Carbamate	11	3	4	10	7	1	11	10	6	1	6	3
Aldicarb_Carbamate	5	2	3	8	12	1	2	10	6	8	9	8
Carbaryl_Carbamate	6	2	6	3	9	2	6	7	15	7	6	5
Diazinon_Organophosphate	1	1	2	0	3	1	3	3	4	30	4	20
Fenobucarb_Carbamate	3	0	4	6	3	1	7	6	12	6	16	9
Pirimicarb_Carbamate	3	0	0	0	2	1	4	10	8	23	10	20

nAChR agonist
cross validation accuracy = 32.6%

	Cyanotropane_cyanotropane	Imidacloprid_neonicotinoid	Levamisole_lev-1 receptor	Nicotine_all nicotinic receptors	SY1134_neonicotinoid	SY1187_neonicotinoid	SY1194_neonicotinoid	Sulfoxaflor_neonicotinoid	Thiamethoxam_neonicotinoid	Monepantel_acr-23 receptor
Cyanotropane_cyanotropane	23	8	2	6	1	7	8	6	6	4
Imidacloprid_neonicotinoid	9	38	7	8	7	3	16	5	3	2
Levamisole_lev-1 receptor	0	4	41	6	0	4	3	4	3	2
Nicotine_all nicotinic receptors	4	11	7	28	4	13	5	10	4	0
SY1134_neonicotinoid	2	14	1	3	13	4	9	1	8	2
SY1187_neonicotinoid	8	6	6	20	4	13	14	7	8	1
SY1194_neonicotinoid	10	10	9	6	16	14	13	9	8	0
Sulfoxaflor_neonicotinoid	7	7	11	9	1	7	11	9	6	1
Thiamethoxam_neonicotinoid	6	4	4	10	3	4	7	9	36	0
Monepantel_acr-23 receptor	2	1	1	0	0	2	2	0	1	32

vAChT inhibitor
cross validation accuracy = 23.3%

	SY1713_spiroindoline-type	SY1727_spiroindoline-type	hemicholinium-3_choline reuptake inhibitor	SY1719_spiroindoline type	SY1769_spiroindoline type	SY1776_spiroindoline type	SY1793_spiroindoline-type	SY1782_spiroindoline-type	SY1783_spiroindoline type	SY1786_spiroindoline type
SY1713_spiroindoline-type	5	4	7	5	3	4	2	6	3	1
SY1727_spiroindoline-type	4	10	6	6	3	3	2	3	6	1
hemicholinium-3_choline reuptake inhibitor	3	5	8	2	0	1	2	1	4	0
SY1719_spiroindoline type	2	2	1	18	8	1	5	9	3	6
SY1769_spiroindoline type	1	1	1	4	7	3	4	7	8	2
SY1776_spiroindoline type	5	1	7	5	5	2	7	3	2	0
SY1793_spiroindoline-type	2	2	3	9	6	1	11	5	4	1
SY1782_spiroindoline-type	1	2	1	8	3	0	3	10	10	5
SY1783_spiroindoline type	7	5	4	3	3	1	7	3	15	8
SY1786_spiroindoline type	2	0	1	7	3	2	5	4	5	13

GABA antagonist
cross validation accuracy = 32.3%

	Dieldrin_orthosteric site	Ethriprole_orthosteric site	Fipronil analogue_orthosteric site	Fipronil_orthosteric site	aryl heterocycle_orthosteric site	Endosulfan_orthosteric site	Endrin_orthosteric site
Dieldrin_orthosteric site	26	9	7	5	10	11	12
Ethriprole_orthosteric site	11	29	15	12	13	3	4
Fipronil analogue_orthosteric site	7	22	14	11	20	8	3
Fipronil_orthosteric site	7	12	20	22	9	1	2
aryl heterocycle_orthosteric site	12	15	9	8	16	6	2
Endosulfan_orthosteric site	12	5	10	3	7	32	9
Endrin_orthosteric site	14	2	2	3	3	8	35

mAChR - agonist
cross validation accuracy = 56.2%

	(±)-Muscarine chloride hydrate _	Arecoline_	Oxotremorine_	oxotremorine-like_	cyclic amine type_
(±)-Muscarine chloride hydrate _	32	18	3	17	8
Arecoline_	20	18	9	12	8
Oxotremorine_	7	4	22	7	18
oxotremorine-like_	22	12	9	36	7
cyclic amine type_	5	5	6	6	153

GluCl agonist
cross validation accuracy = 27.6%

	Doramectin_mectin	Emamectin benzoate_mectin	Ivermectin_mectin	Avermectin B2a_mectin	Avermectin type_mectin
Doramectin_mectin	8	13	0	2	5
Emamectin benzoate_mectin	9	15	2	7	5
Ivermectin_mectin	2	3	2	2	3
Avermectin B2a_mectin	1	7	3	5	7
Avermectin type_mectin	4	10	0	4	4

Octopamine agonist
cross validation accuracy = 43.5%

	SY1382_oxazoline	Amitraz_amidine	Octopamine_octopamine	SY1344_thiazoline	SY1361_thiazoline	SY1392_oxazoline	imidazoline_imidazoline	thiazoline_thiazoline
SY1382_oxazoline	48	0	1	3	1	13	8	3
Amitraz_amidine	0	7	11	4	1	5	13	2
Octopamine_octopamine	0	5	26	7	0	9	34	5
SY1344_thiazoline	3	5	8	19	0	12	9	10
SY1361_thiazoline	0	1	0	1	33	4	14	2
SY1392_oxazoline	4	0	4	2	0	7	5	4
imidazoline_imidazoline	2	10	29	6	10	34	142	18
thiazoline_thiazoline	8	5	2	7	4	13	31	20

Tubulin - depolymeriser
cross validation accuracy = 32.5%

	Butralin_inhibits polymerisation	colchicine_	SY1559_inhibits polymerisation	Thiophanate-methyl_inhibits polymerisation	Benomyl_depolymeriser
Butralin_inhibits polymerisation	25	10	10	9	12
colchicine_	18	21	12	9	8
SY1559_inhibits polymerisation	13	16	20	12	10
Thiophanate-methyl_inhibits polymerisation	12	8	21	19	14
Benomyl_depolymeriser	18	6	11	12	31

Figure EV3. Confusion matrices showing cross-validation performance of a classifier trained to distinguish compounds of the same class from each other.

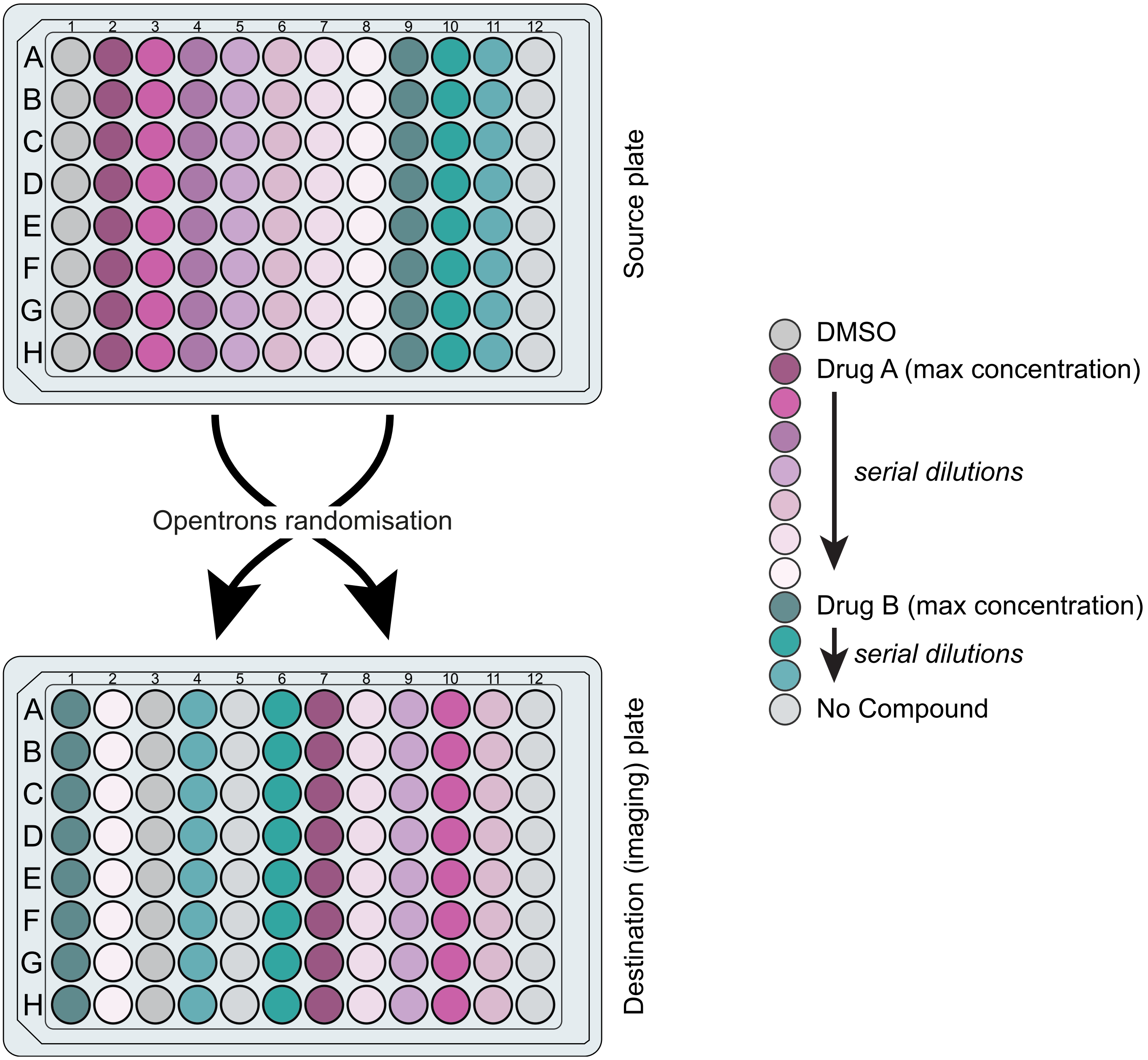

Figure EV4. Randomization of columns using liquid handling robot.

To minimize any position-induced bias, we use an Opentrons liquid handling robot to randomly shuffle the position of the compounds in the imaging plates. We programmed the robot to keep a record of the randomized shuffle and use this log to create the correct well-compound mapping.

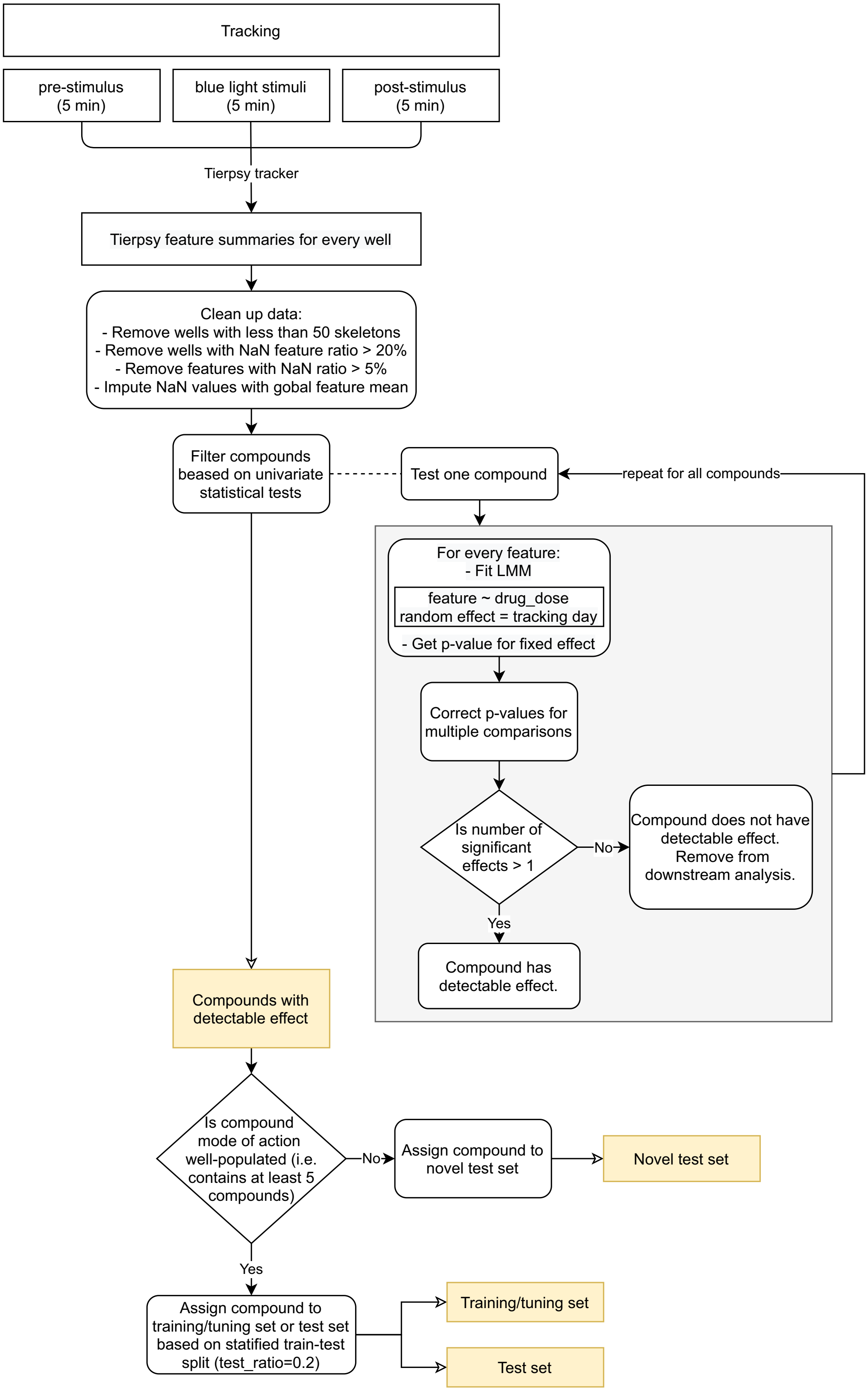

Figure EV5. Flow chart showing the data pre-processing steps.

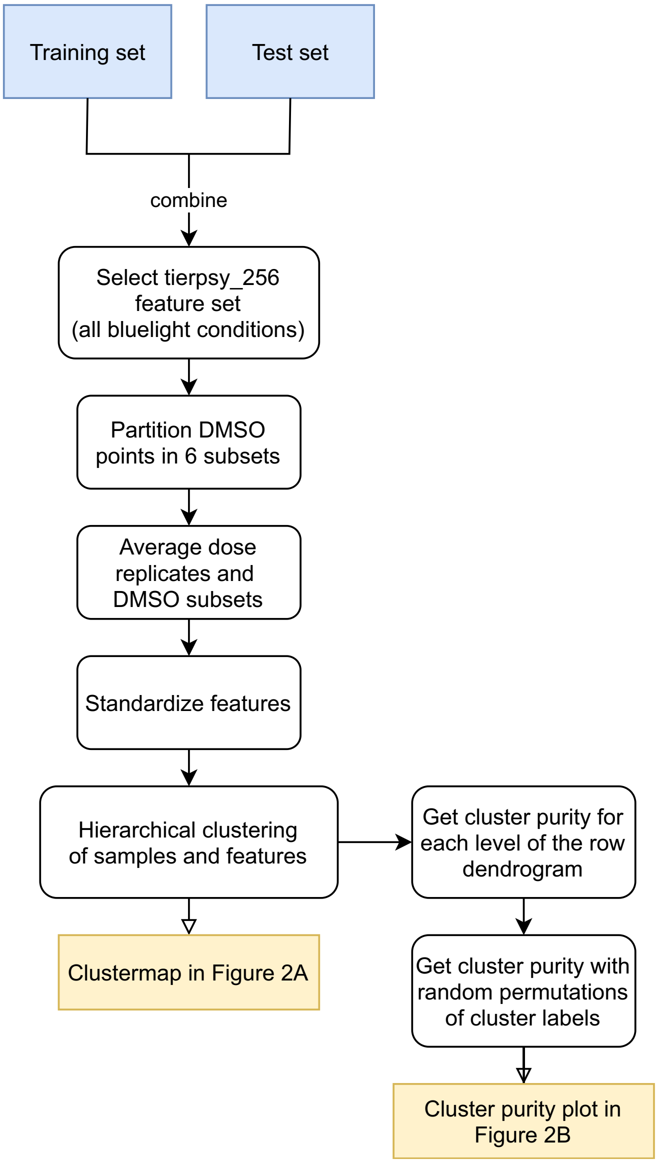

Figure EV6. Flow chart showing the pipeline for the clustering of average drug doses.

Figure EV7. Flow chart showing the steps followed for the tuning and training of the classifier using the training dataset and the prediction of the mode of action in the test set.

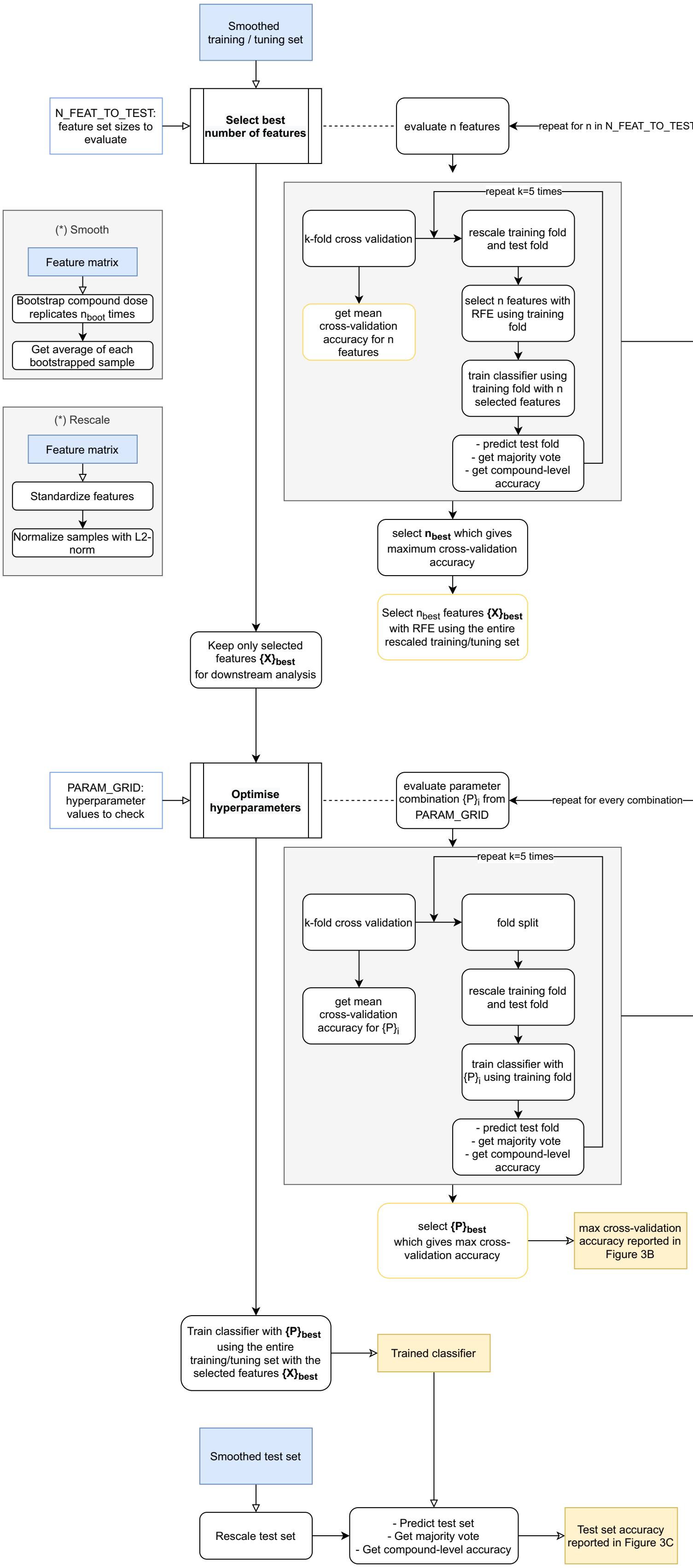

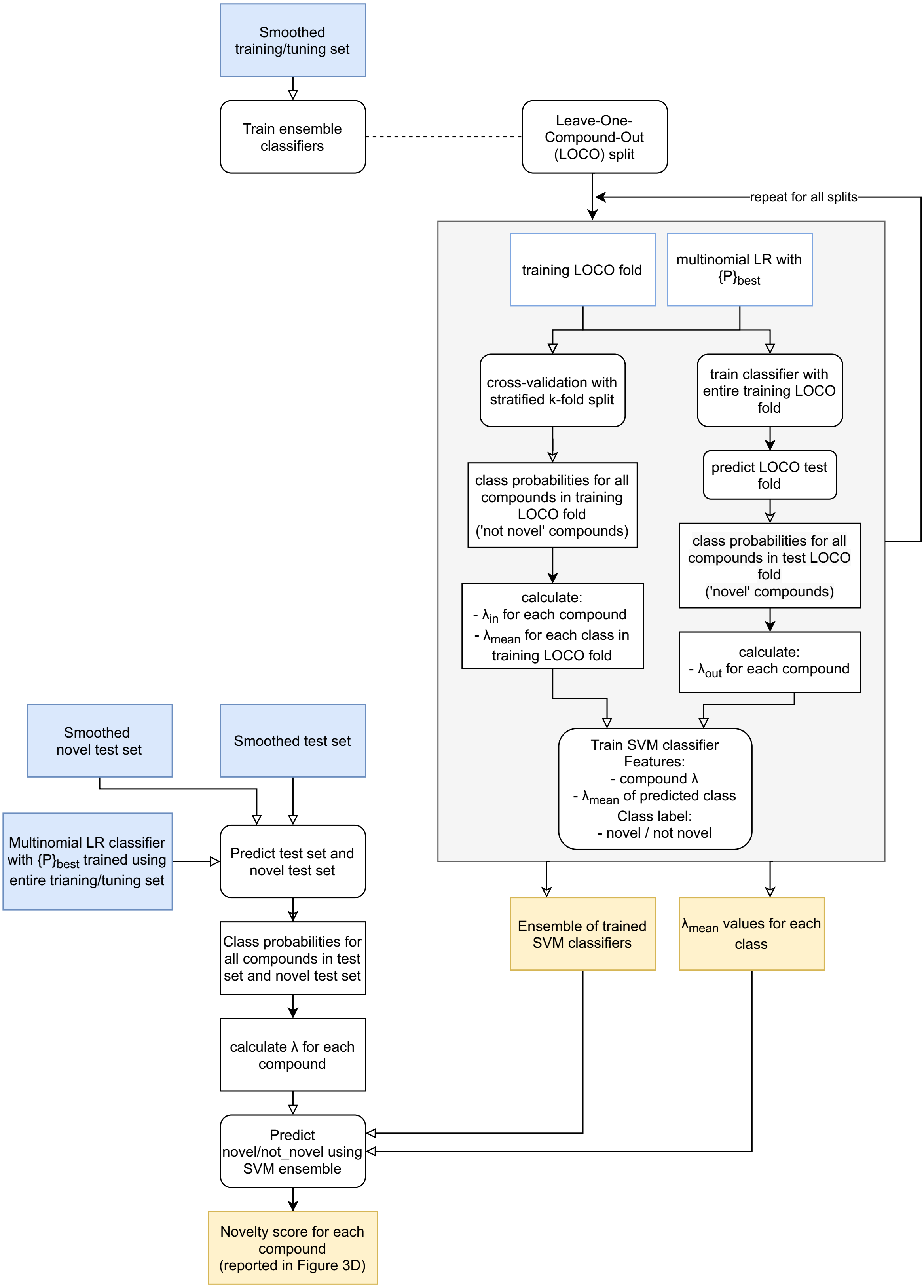

Figure EV8. Flow chart showing the steps of the novelty detection method.